# PS Permeability Prediction and Distribution in the Confined South Georgia Rift Red Beds With Implications for $CO_2$ Storage*

**Olusoga M. Akintunde[1], Camelia C. Knapp[2], and James H. Knapp[2]**

Search and Discovery Article #80590 (2017)**
Posted May 8, 2017

*Adapted from poster presentation given at AAPG 2017 Annual Convention and Exhibition, Houston, Texas, April 2-5, 2017

[1]TGS, Houston, Texas, United States (olusogamartins@gmail.com)
[2]School of the Earth, Ocean, and Environment, University of South Carolina, Columbia, South Carolina, United States

## Abstract

The lack of a permeability log necessary to assess reservoir injectivity as well as aid the correlation and interpretation of existing porosity and resistivity logs for reservoir quality characterization for $CO_2$ storage in the South Georgia Rift red beds provides the motivation for this study. $CO_2$ sequestration seems to be the most viable near-term solution to global warming. Besides, the significant cost ($10M - $100M) associated with drilling and logging for in situ permeability coupled with the limited resolution of existing core data further makes this work compelling. Knowledge of permeability will also aid dynamic reservoir modeling of the distribution of fluid flow to better characterize the $CO_2$ injection distribution and efficiency for the purpose of storage optimization and management. We applied a methodology that utilizes the pore space and geohydraulic properties of the reservoir from existing laboratory and well data to produce a newly derived permeability log. It shows non-uniform distribution with depths possibly due to reservoir response and sensitivity to geologic changes in the confined and heterogeneous red beds. It also manifests characteristics consistent with observations from the porosity and resistivity logs. The interpretation of these logs provides evidence for the presence of low permeable, tightly cemented, and compacted red beds. The regional significance of this is that the South Georgia Rift red beds and possibly the ones encountered in other buried Triassic-Jurassic basins in the Southeastern United States are most likely to be low permeable rocks in view of the similarities in age, geologic history, and composition. We conclude that while the low permeability aided by the low resistivity depicted in the red beds suggests increased confining stress and reduced injectivity, any pore pressure increase with $CO_2$ injection over time may counteract these thereby opening pores for improved injectivity.

## References Cited

Akintunde, O.M., C.C. Knapp, and J.H. Knapp, 2013, Petrophysical Characterization of the South Georgia Rift Basin for Supercritical $CO_2$ Storage: A Preliminary Assessment: Environmental Earth Sciences, v. 70, p. 2971-2985.

Amaefule, J.O., M. Altunbay, D. Tiab, D.G. Kersey, and D.K. Keelan, 1993, Enhanced Reservoir Description: Using Core and Log Data to Identify Hydraulic (Flow) Units and Predict Permeability in Uncored Intervals/Wells: 68th Annual Technical Conference and Exhibit, Houston, TX, SPE26435.

Gohn, G.S., B.B. Houser, and R.R. Schneider, 1983, Geology of the Lower Mesozoic (?) Rocks in Clubhouse Crossroads Test Hole #3 Near Charleston, South Carolina, *in* G.S. Gohn (ed.), Studies Related to the Charleston, South Carolina, Earthquake of 1886 - Tectonics and Seismicity: US Geological Survey Professional Paper 1313, p. D1-D17.

Gomez, T.C., J. Dvorkin, and T. Vanorio, 2010, Laboratory Measurements of Porosity, Permeability, Resistivity, and Velocity on Fontainebleau Sandstones: Geophysics, v. 75/6, p. E191-E204.

Heffner, D.M., J.H. Knapp, O.M. Akintunde, and C.C. Knapp, 2012, Preserved Extent of Jurassic Flood Basalt in the South Georgia Rift: A New Interpretation of the J Horizon: Geology, v. 40/2, p. 167-170.

McBride, J.H., K.D. Nelson, and L.D. Brown, 1989, Evidence and Implications of an Extensive Early Mesozoic Rift Basin and Basalt/Diabase Sequence Beneath the Southeast Coastal Plain: Geological Society of America Bulletin, v. 101, p. 512-520.

# Permeability Prediction and Distribution in the Confined South Georgia Rift Red Beds with Implications for $CO_2$ Storage

Olusoga M. Akintunde*, Camelia C. Knapp**, and James H. Knapp**
* TGS, Houston, Texas; **School of the Earth, Ocean, and Environment, University of South Carolina, Columbia, SC 29208, USA

## Introduction and Motivation

## Geologic History and Tectonics

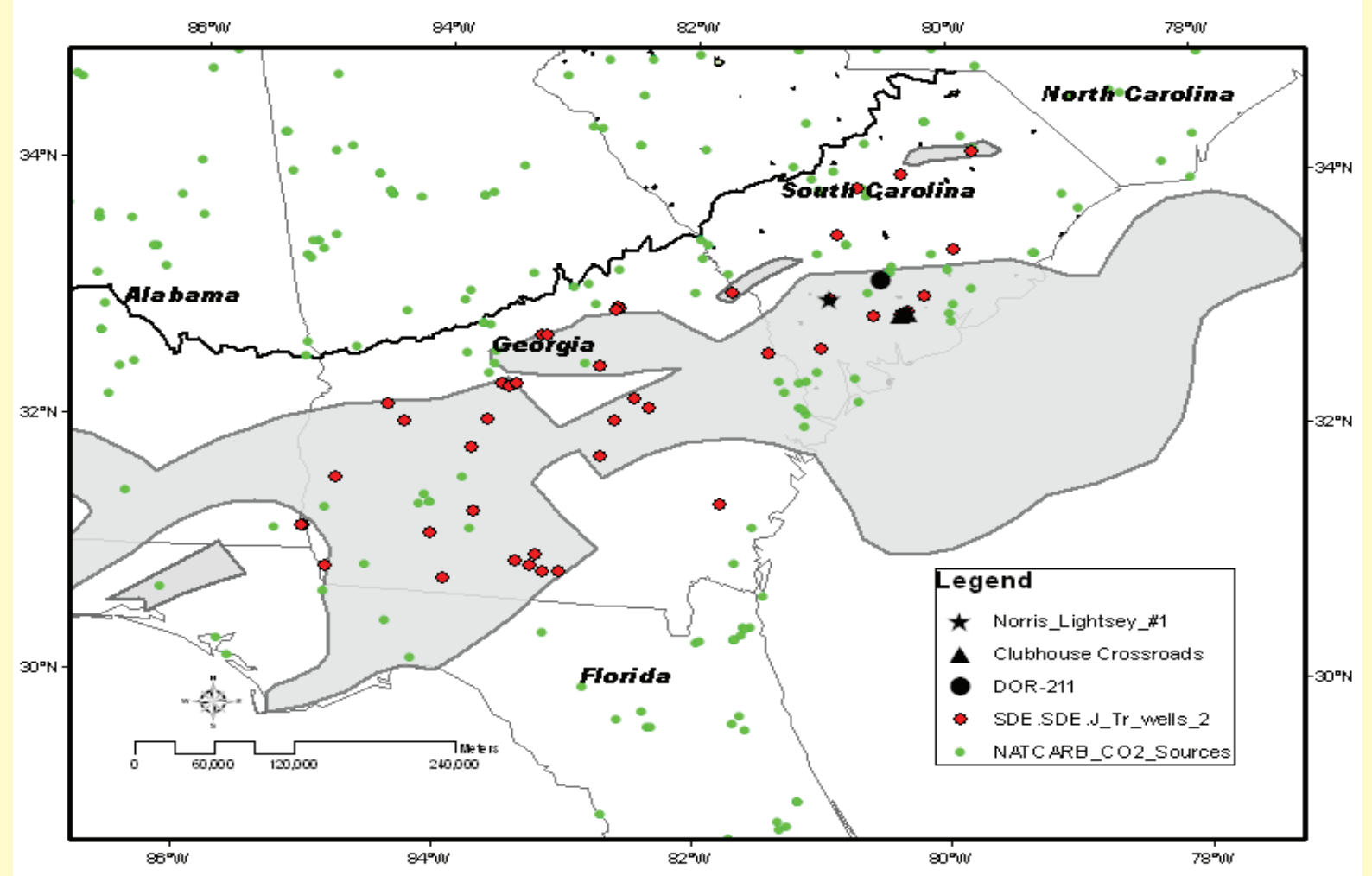

Figure 1. South Georgia Rift (SGR) basin (McBride et al., 1989; Heffner et al., 2012)

The SGR basin was formed around 215-175 Ma.
Deposition of Triassic sediments occurred in late Triassic-Early Jurassic (Gohn et al., 1983).
Basalt and diabase accompanied rifting at 170 Ma.
Thickness of basin-fill is about 3.5 km.
SGR is perhaps the largest and most geologically coplex Mesozoic half-graben of Eastern North America Margin

1. The SGR contains porous red beds and other features that make it attractive for $CO_2$ storage evaluation
2. This study focuses on the Norris Lightsey red beds
3. Lack of a permeability log necessary for reservoir injectivity and quality assessment motivated this study
4. New drilling & logging could cost \$10M - \$100M
5. Existing core permeability data are limited in resolution

## The Norris Lightsey well logs

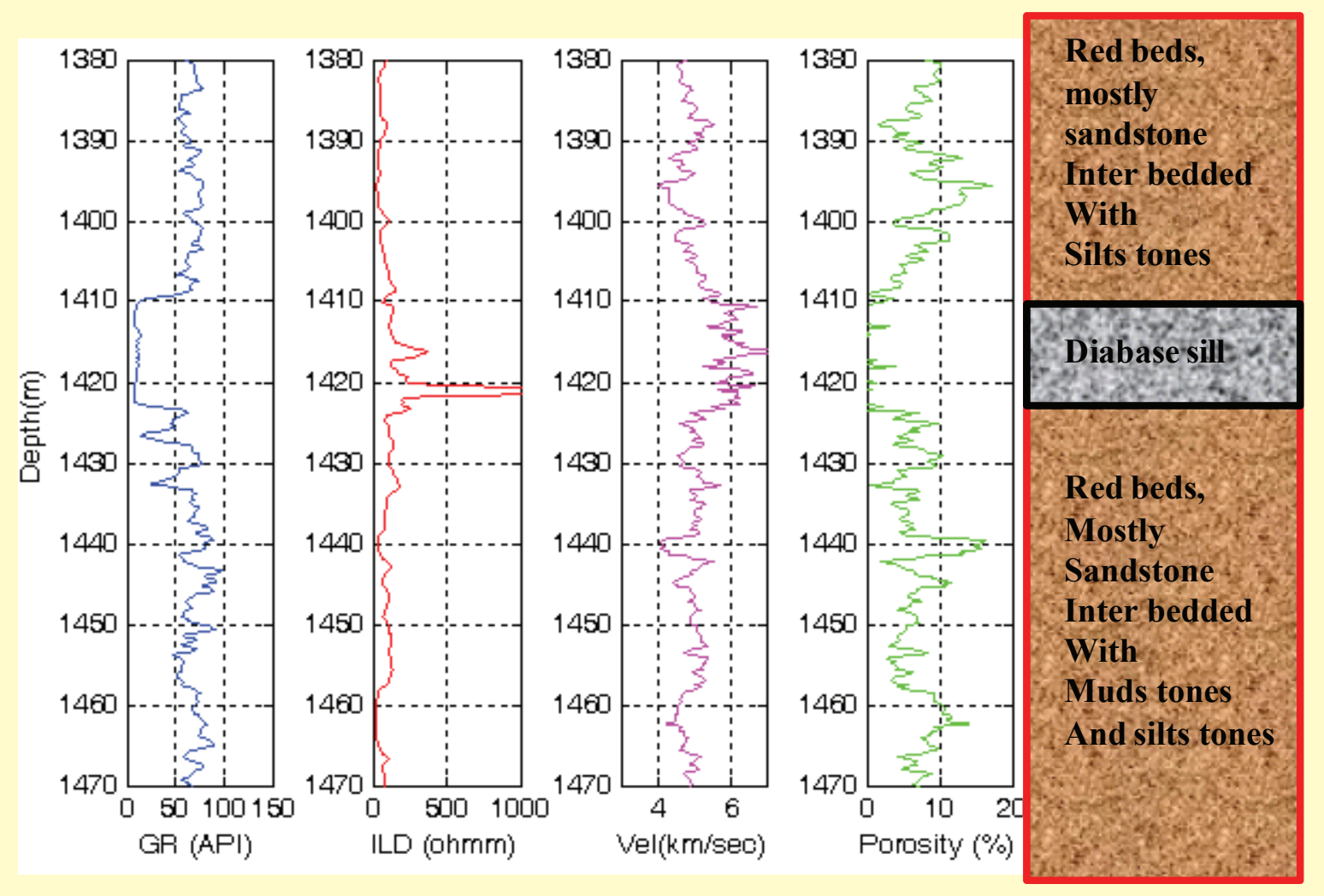

## Composition & Characteristics of the Red Beds

1. Coarse to fine-grained that are poorly-sorted
2. Mudstone, claystone, and conglomerate clasts
3. Texturally and compositionally immature

Figure 2. Red beds from CC-3 well. These share similar lithology with the Norris Lightsey (Akintunde et al., 2013)

## Petrographical Analysis

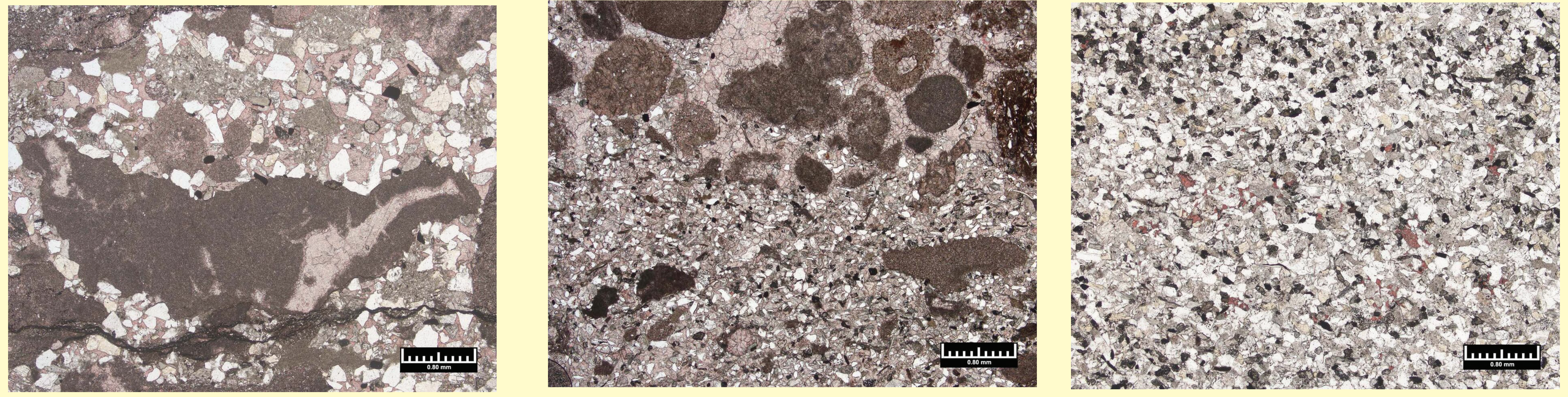

Figure 8:Thin sections of red beds at 1172 m, 1602 m, and 1773 m recovered from the Rizer #1 test borehole about 5 miles from Norris Lightsey (Weatherford Lab. Report, 2014).

## Objectives of Study

1. Understand permeability changes with depth
2. Investigate how these changes may impact
   (A) reservoir injectivity
   (B) reservoir quality
   (C) success and safety of $CO_2$ injection, and
   (D) the suitability of SGR for long-term storage

Table 1: Core lab-derived porosity and permeability data

| S/N | Sample ID | Depth (m) | Porosity (%) | Permeability (mD) | Source (year) |
|---|---|---|---|---|---|
| 1 | Sumter | 213.06 | 10.6 | 0.16 | This study: WL (2011) |
| 2 | Berkeley_1 | 548.34 | 13.3 | 0.15 | This study: WL (2011) |
| 3 | Berkeley_1a | 548.34 | 13.0 | 0.10 | This study: CSM (2011) |
| 4 | Berkeley_2 | 556.56 | 8.6 | 0.01 | This study: WL (2011) |
| 5 | Berkeley_2a | 556.56 | 8.9 | 0.01 | This study: CSM (2011) |
| 6 | Durbarton | 821.13 | 6.3 | 0.016 | Marine and Siple (1974) |
| 7 | CC-3* | 987.86 | 2.6 | 0.001 | This study: WL (2012) |
| 8 | CC-3* | 988.47 | 2.1 | 0.0023 | This study: WL (2012) |
| 9 | Norris Lightsey_1 | 1,040 | 22.6 | 1.5 | CL (1984) |
| 10 | Norris Lightsey_2 | 1,059.2 | 23.8 | 2.2 | CL (1984) |
| 11 | Norris Lightsey_3 | 1,505 | 24.2 | 6.7 | CL (1984) |
| 12 | Norris Lightsey_4 | 1,522 | 27.7 | 3.7 | CL (1984) |
| 13 | Norris Lightsey_5 | 1,047 | 28.1 | 8.9 | CL (1984) |
| 14 | Norris Lightsey_6 | 1,146 | 32.5 | 6.9 | CL (1984) |

## Results of Permeability Prediction and Analysis

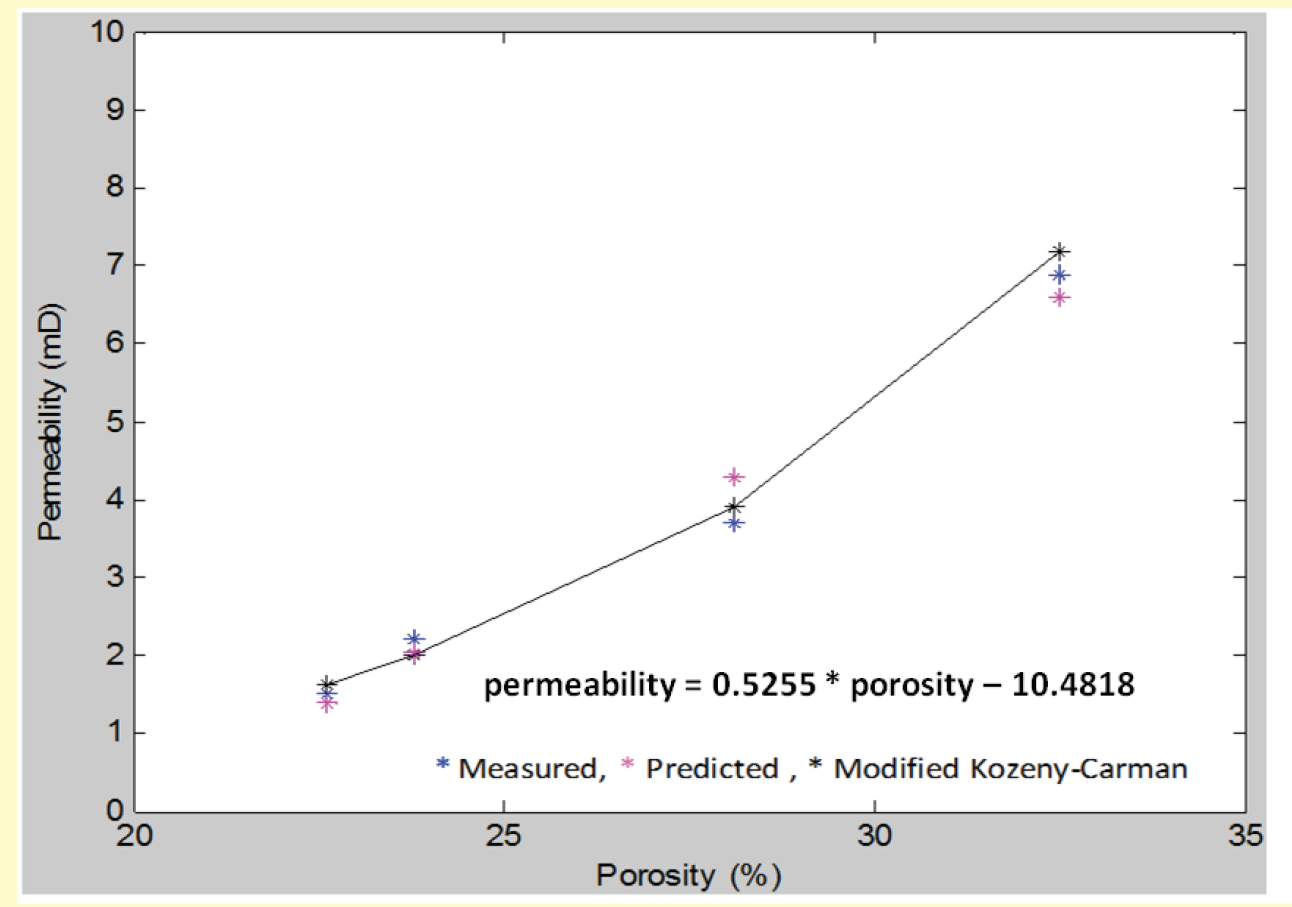

Figure 4. Permeabilty-porosity relationship

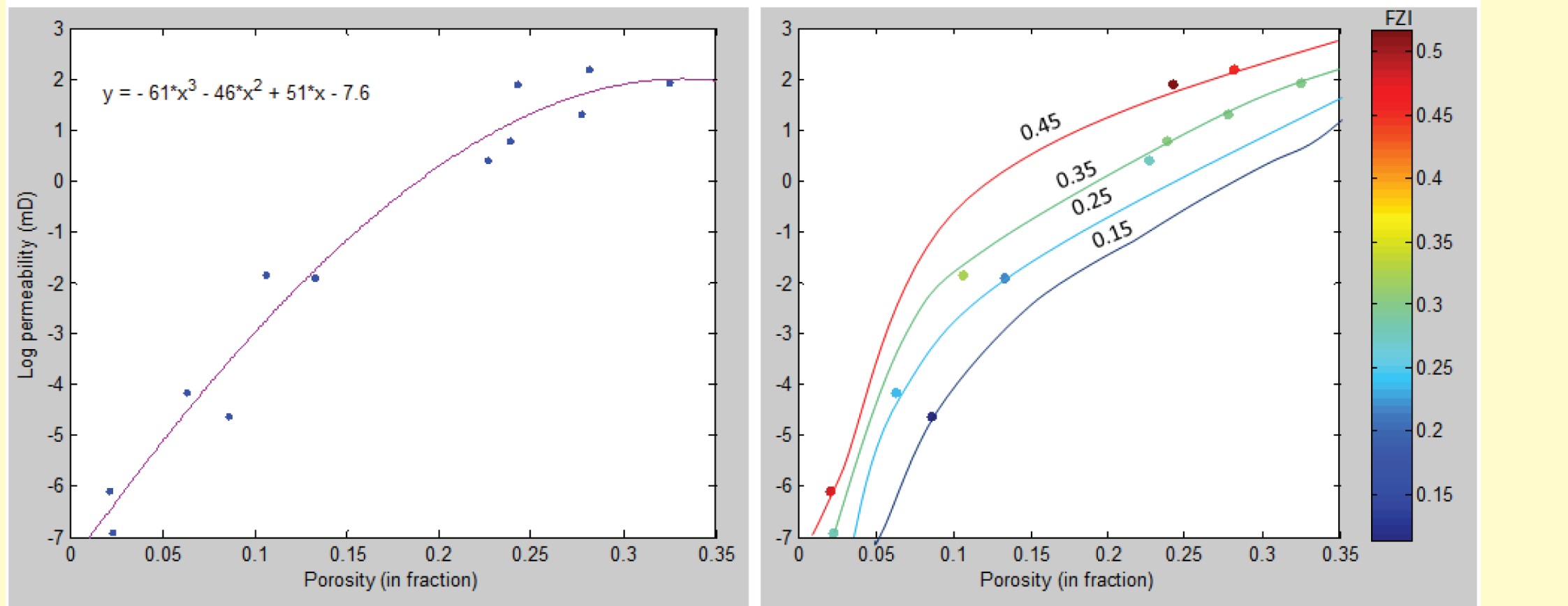

Figure 5. Permeability-porosity distribution from FZI units

## Key Observations

1. The observed consistency in the trends of the porosity and permeability logs validate the reliability of prediction
2. The low permeablity relative to porosity shows that permeability is also dependent on the gemoetric properties of the rock
3. We interpret the non-uniform permeability distribution in conjunction with thin sections analysis to be due primarily to geologic changes
4. While low permeability would reduce injectivity, continuing $CO_2$ injection may open closed pores for enhanced, dynamic permeability
5. The potential for long-term $CO_2$ storage in the SGR red beds would rest on safe, systematic implementation of a dynamic permeability storage system

## Materials and Methods

1. Use of existing well and core laboratory data (Table 1)
2. Development of porosity-permeability transform
3. Computation of Flow Zone Indicators (FZI) from Table 1
4. Convert the given porosity log to a permeability log
   (A) using the derived porosity-permeability transform, and (B) the computed FZI units

## Governing Equations

$$(1)\quad k = \left(\frac{d_{Mean}^2}{72\tau^2}\right)\frac{(\phi-\phi_p)^3}{[1-(\phi-\phi_p)]^2}$$

$$(2)\quad FZI = \frac{0.0314}{\epsilon}\sqrt{\frac{k}{\phi}}$$

$$(3)\quad \epsilon = \frac{\phi}{1-\phi}$$

(1) Kozeny-Carman relation (Gomez et al., 2010)
(2) Flow Zone Indicator (Amaefule et al., 1993)
(3) Ratio of pore volume to grain volume

## Newly developed permeability log

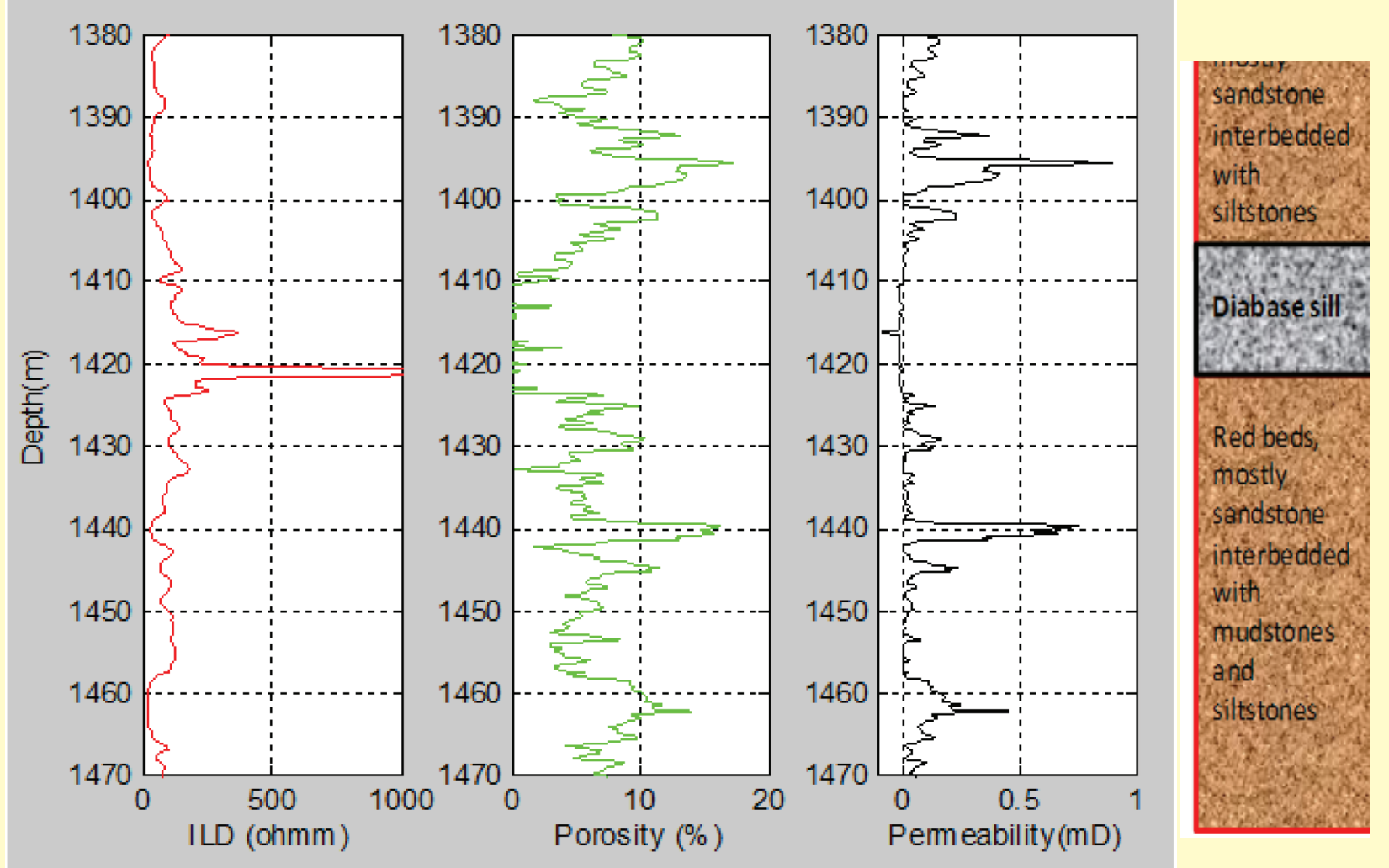

Plotted along side are resistivity and porosity logs. Porosity and permeability logs exhibit similar trends

Figure 5. The derived permeability log (top most right)

## Conclusions

1. A robust methodology involving FZI and Kozeny-Carman was applied to develop a permeability log for the study area
2. The interpreted low permeability aided by thin sections indicate cemented, compacted red beds with increasing confining stress
3. Analysis suggests the implementation of a dynamic permeability $CO_2$ storage system for the study area
4. Dynamic reservoir modeling and field testing of the enhanced permeability approach are recommended

**Acknowledgements:** This work was supported by the United States Department of Energy (DOE) under Award Number DE-FE0001965.
We thank John Shafer, Mike Waddell, Adrian Addison, Duke Brantley, Mark Evans, Bill Clendenin, Scott Howard, and David Heffner for their contributions.

Thin sections were provided by Weatherford Laboratories. We also thank Prof. Manika Prasad of the Colorado School of Mines for access to their Rock Physics Laboratory.